Interdisciplinary Modeling and Dynamics of Archipelago Straits

Dr. Pierre F.J. Lermusiaux
Department of Mechanical Engineering, Center for Ocean Science and Engineering,
Massachusetts Institute of Technology; 5-207B; 77 Mass. Avenue; Cambridge, MA 02139-4307
phone: (617) 324-5172   fax: (617) 324-3451   email: pierrel@mit.edu

LONG-TERM GOALS

The general focus of this work is to explore, better understand, model and predict the interactive dynamics and variability of sub-mesoscale and mesoscale features and processes in the Philippine Straits region and their impacts on local ecosystems through

  i. physical-biogeochemical-acoustical data assimilation of novel multidisciplinary observations,

 ii. adaptive, multi-scale physical and biogeochemical modeling,

iii. process, sensitivity studies based on a hierarchy of simplified simulations and focused modeling.

OBJECTIVES

- Utilize and develop systems for interdisciplinary data assimilation and uncertainty estimation with the physical Primitive-Equation (PE) and generalized biogeochemical model of the Multidisciplinary Simulation, Estimation, and Assimilation Systems (MSEAS) group

- Study, describe and model the variability and dynamics of flow separations and associated eddies and filaments, of water mass evolutions and pathways, and of locally trapped waves

- Develop and implement schemes for parameter estimation and selection of model structures and parameterizations, and for high-resolution nested domains towards non-hydrostatic modeling

APPROACH

The technical approach is based on multiscale (tidal-to-large-scales) ocean dynamical modeling with free-surface primitive equation models and tidal forcing. It involves data assimilation with ESSE, quantitative model evaluation and selection, and sensitivity and dynamical process studies.

The ongoing physical and biogeochemical scientific research focuses on:

- Data assimilation (DA) of novel multidisciplinary data types, especially remotely sensed data.

  - measurement models and interdisciplinary DA: investigate multi-grid DA/ESSE combination

  - high-resolution DA: assimilate sub-inertial processes and interactions without aliasing

1. REPORT DATE **2010**	2. REPORT TYPE	3. DATES COVERED **00-00-2010 to 00-00-2010**

4. TITLE AND SUBTITLE	5a. CONTRACT NUMBER
Interdisciplinary Modeling and Dynamics of Archipelago Straits	5b. GRANT NUMBER
	5c. PROGRAM ELEMENT NUMBER
6. AUTHOR(S)	5d. PROJECT NUMBER
	5e. TASK NUMBER
	5f. WORK UNIT NUMBER

7. PERFORMING ORGANIZATION NAME(S) AND ADDRESS(ES) **Massachusetts Institute of Technology,Department of Mechanical Engineering,Center for Ocean Science and Engineering,Cambridge,MA,02139-4307**	8. PERFORMING ORGANIZATION REPORT NUMBER

9. SPONSORING/MONITORING AGENCY NAME(S) AND ADDRESS(ES)	10. SPONSOR/MONITOR'S ACRONYM(S)
	11. SPONSOR/MONITOR'S REPORT NUMBER(S)

12. DISTRIBUTION/AVAILABILITY STATEMENT
Approved for public release; distribution unlimited

13. SUPPLEMENTARY NOTES

14. ABSTRACT

15. SUBJECT TERMS

16. SECURITY CLASSIFICATION OF:			17. LIMITATION OF ABSTRACT	18. NUMBER OF PAGES	19a. NAME OF RESPONSIBLE PERSON
a. REPORT **unclassified**	b. ABSTRACT **unclassified**	c. THIS PAGE **unclassified**	**Same as Report (SAR)**	**17**	

- Process and sensitivity studies

  ○ processes: variability and dynamics of flow; pathways and transformation of water masses; tidal – buoyancy flow interactions; biological responses; blooms; biological accumulations

  ○ model-based studies: sensitivity studies; term and flux balances and transports; energy diagnostics; estimation of dominant scales of variability; predictability

- Physical and biogeochemical modeling including: adaptive modeling, tidal modeling and multi-dynamics nested domains and non-hydrostatic modeling

WORK COMPLETED

Realistic Multiscale Simulations and Dynamics

Modeling System Improvements: As a result of the geographic complexity of the Philippines Archipelago, very significant model improvements were necessary prior to, during and after the three real-time experiments. Various model parameters (bottom friction, mixing, etc.) were tuned, but more importantly, new methods were developed and software built for complex archipelagos with topographic barriers and multiply-connected domains. These include new schemes for: i) objective mapping using Fast Marching Methods (Agarwal, 2009; Agarwal and Lermusiaux, 2010); ii) optimizing the many inter-island transports in initializations from geostrophic shear (Agarwal et al., 2010); iii) region-dependent biological initialization; iv) multiscale fully implicit two-way nesting (Haley and Lermusiaux, 2010); and iv) generalized inversion for high-resolution barotropic tidal fields (Logutov and Lermusiaux, 2008). Without such schemes, this region could not be adequately modeled.

*Modeling Domains and Bathymetry***:** For the Philippines Experiment (PhilEx) region**,** we employ spherical coordinates and six 2-way nested domains in telescoping set-ups, ranging from a 3267x3429 km regional domain at 27 km resolution down to a pair of roughly 170x220 km strait domains with 1km resolution (Fig. 1). Simulations performed to date are primarily for the Feb-Mar 2009 period, focusing on the 1656x1503 km Archipelago domain (9 km resolution), the 552x519 km Mindoro Strait domain (3 km resolution) and the 895x303 km Mindanao domain (3 km resolution). All domains have 70 vertical levels in a double-sigma configuration, optimized for the local steep bathymetry and depths of thermoclines/haloclines. We found that V12.1 of the Smith and Sandwell (SS, 1997) topography was not always accurate; at times too shallow compared to the depth of ocean measurements or very different from ship bathymetric data. As topography is a key variable for the dynamics in the region, we updated the V12.1 topography with bathymetry extracted from hydrographic profile data and ship bathymetry and hydrographic data. Specifically, we replaced the SS data if the hydrographic data were deeper or if ship bathymetry data was available; solving a local diffusion equation (MSEAS Group, 2010) to merge data sources and ensure bathymetric continuity.

*Initial and Boundary Conditions***:** Simulations were initialized using NODC World Ocean Atlas 2005 (WOA05) climatological profiles. WOA05 profiles for February were used for the 0-1500m depth range and winter profiles were used from 1500m to the bottom. The profiles were gridded using a new objective analysis scheme (Agarwal and Lermusiaux, 2010) which computes the length of shortest sea paths among model and data points using the Fast Marching Method (FMM) and then uses these distances in the covariance models. Since the NODC database does not contain any CTD observations in February, the WOA05 climatology provides an estimate of the salinity of the Sulu Sea in February which is an unrealistic mixture of surrounding water masses. It was necessary to correct for this, using

our new objective analysis and initialization schemes. Specifically, as one of our goals is to utilize only historical data, we initialized our re-analysis for February in the Sulu Sea using historical CTD data for the month of March. This ensures that Sulu Sea water masses are in the Sulu Sea. The same situation occurs for the Bohol Sea and we had to proceed similarly. For surface boundary conditions, in real-time, we employed COAMPS fluxes for wind stress and NOGAPS fluxes for net heat flux and evaporation-minus-precipitation. Subsequently, extensive evaluations of atmospheric forcing surface fluxes were completed and for the re-analysis results, COAMPS archive fluxes for wind stress, net heat flux and evaporation-minus-precipitation are employed.

Idealized Simulations and Dynamics with Finite Element Methods

We have further improved upon our previously developed 2D-in-space Discontinuous Galerkin Finite Element (Reed and Hill, 1973) MATLAB framework (Ueckerman, 2009). Specifically, for idealized simulations in strait regions, we completed comprehensive numerical analyses, employing standard and hybrid discontinuous Galerkin Finite Element Methods (Cockburn et al, 2009, and Nguyen et al., 2009), on both straight and new curved elements (Ueckermann and Lermusiaux, 2010). Our analyses focused on nutrient-phytoplankton-zooplankton dynamics under advection and diffusion within an ocean strait, in an idealized two-dimensional geometry. This allowed us to complete a large number of sensitivity studies which we synthesized. For the dynamics, we investigated three biological regimes, one with single stable points at all depths and two with stable limit cycles. We also examined interactions that are dominated by the biology, by the advection, or that are balanced. For these regimes and interactions, we study the sensitivity to multiple numerical parameters including: quadrature-free and quadrature-based discretizations of the source terms; order of the spatial discretizations of advection and diffusion operators; order of the temporal discretization in explicit schemes; and resolution of the spatial mesh, with and without curved elements.

We also described the physical and biological features predicted in real-time as well as tidal fields (Lermusiaux et al, 2011). We also compared the forecast features to in situ and satellite data.

RESULTS

Realistic Multiscale Simulations and Dynamics

We utilized our multi-resolution modeling system to study multiscale dynamics in the region, without the use of any synoptic *in situ* data, so as to evaluate modeling capabilities when only sparse, remotely sensed, sea surface height data is available for assimilation. We focused on the Feb-Mar 2009 period and compared our simulation results to ocean observations. The oceanographic findings include: a description of the main circulation features, the evolution of flow fields within three major straits, the estimation of transports to and from the Sulu Sea and the corresponding balances, and finally, an investigation of multiscale mechanisms involved in the formation of the deep Sulu Sea water.

Circulation Features: Model estimates of the ocean currents and salinity fields averaged over a selected set of depth ranges and over time during 18-25 February 2009 and during 18-25 March 2009 are utilized to provide a description of the main circulation features within the Philippine Archipelago (Fig. 2). A synopsis of that description is provided here, while the complete analysis can be found in Lermusiaux et al. (2011). From the Pacific Ocean, the North Equatorial Current impinges upon the Philippine Archipelago, splitting into two boundary currents: the equatorward Mindanao current and the northward Kuroshio (Fig. 2a). Part of the Mindanao current flows along the island of Mindanao

into the eastern Sulawesi Sea (Fig. 2b). The Mindoro Strait system (Fig. 2c-e) provides a connection for the South China Sea to the Sulu Sea (through the Panay Sill) and to the Sibuyan Sea (through the Tablas Strait). Near-surface flow in the Mindoro/Panay Straits begins southward on average in February (Fig. 2c) but reverses to a northward average for last part of February and March (Fig. 2e). At depth, the flow is predominantly southward (Fig. 2d), weaker at mid-depth and much stronger near the bottom. At the mouth of the Panay Sill, the cyclonic surface Panay eddy is present for mid-to-late February (Fig. 2c) before being mostly absorbed into northward surface flow (Fig. 2e). The Sibuyan Sea has a direct connection to the Pacific Ocean through the San Bernardino Strait. Although tidally active, the mean flows through the strait are negligible (Fig. 2c-e). In the Bohol, the upper 100m time/depth averaged fields show an inflow from the Pacific through the Surigao Strait into the Bohol, joining the Bohol jet along the northern edge of the Bohol (Fig. 2f). This jet continues through the Dipolog Strait into the Sulu Sea joining a cyclonic eddy and proceeding northward along Negros Island. In the western Bohol, the southern edge of the Bohol jet merges with the cyclonic Iligan Bay eddy (Fig. 2f). At 400-500m the flow through the Dipolog strait is eastward from the Sulu Sea into the Bohol Sea (Fig. 2g). At intermediate depths, the flow through Dipolog is more variable. The Sulu Sea has a fairly complex eddy field with a general cyclonic flow. On average the Sulu Sea has a net inflow from the Balabac, Mindoro/Panay and Dipolog straits and net outflow through the Sibutu Strait and the Sulu archipelago. Although the Sibutu Strait has a net outflow, it is tidally active and experiences episodic net inflows from the Sulawesi (especially in the bottom layers). Sibutu Strait tides generate strong internal tides and waves. Strong internal tides and waves also occur along the southern rim of the Sulu Sea by the western half of the Sulu archipelago steep shelfbreak. Smaller but appreciable internal tides/waves occur along the western edge of the Sulu Sea from Borneo to the Balabac Strait to Palawan Island. These sites provide a mixing mechanism for the generation of Sulu deep water.

Flows within Straits and Transports to the Sulu Sea: We compare the time-series of measured and simulated along-strait velocities at the Panay (Fig. 3a,d), Mindoro (Fig. 3b,e) and Dipolog (Fig. 3c,f) moorings. Our simulated flows through the straits proper are in generally good agreement with the strength, direction and structure of the observed flows; e.g. the bottom intensified flows at Panay and Dipolog. This is a significant result since many factors could lead to large differences, including: (i) the lack of synoptic *in situ* data in the simulation; (ii) local bathymetry is very tortuous, uncertain and only simulated at 3km resolution; and iii) assimilation of SSH every three days to one week does not resolve strait flows. In Figure 4, we compare the time-averaged values of the above velocity profiles, providing now both the along-strait and across-strait time-averaged velocities. The time-averaged mean profiles confirm all of the along-strait findings shown on Fig. 3. More surprising is that even the across-strait mean flows are relatively well captured, although the nested-domain resolution is still too coarse for these smaller scales processes, in part controlled by each strait's width, which can be very narrow at depth. It is only for the deep Dipolog that the shape of the across-strait flow is off, perhaps due to the sharp meanders of the strait at depth, not represented in the 3km model bathymetry.

The above comparisons are at single mooring positions located at the expected sills of each strait, chosen to measure the deepest overflows. To extend these results, we also examined the overall water transports across sea segments between islands. To accurately estimate the transports into and out of the Sulu Sea, we employ an algorithm consistent with the conservation of mass imposed by our nonlinear free surface model (eqn. 65 in Haley and Lermusiaux, 2010). The transport along a line segment is the integral of the terms in the divergence operator along model grid edges that best approximate the given line segment. To find that set of grid edges, we employ the Bresenham (1965) line algorithm. The resulting transports are plotted as functions of time in Figs. 5b-f (positive outward),

for each of the five open-sea segments surrounding the Sulu Sea (Fig. 5a). We determine time-averaged mean flows of: Sulu Archipelago – 3.47 Sv outflow; Mindoro strait – 1.65 Sv inflow; Balabac Strait – 1.04 Sv inflow; Diplolog strait – 0.79 Sv; and, the Guimaras Strait – essentially no net flow (8×10^{-4} Sv). Summing the inflows of the four sections provides a mean 3.48 Sv inflow. The difference between the mean inflow and mean outflow is a net 0.01 Sv inflow; equal to the free-surface term in our model equations and equivalent to a mean 3mm rise in the Sulu SSH over a time step of 150sec. Based on the ensemble of simulations run, the mean transport uncertainties are about 50%.

Deep Sulu Sea Water: In the Sulu Sea below 1250m, salinity is observed to be slightly stratified from a minimum of 34.45 to 34.744, while the temperature is relatively uniform, suggesting that the deep water is a mixture of water masses. We have examined the multiscale processes likely responsible for this deep water formation. The two deepest straits leading to the Sulu Sea are the Panay Sill to the northeast (depth of sill around 570m) and Sibutu Strait to the southwest (depth of sill near Pearl Bank around 370m). We show their location (Fig. 6a) and the corresponding deep transports as a function of time (Figs. 6b,d). We find a net time-average deep inflow of 0.645 Sv over the Panay Sill to the Sulu (Fig. 6b), with a 50% uncertainty standard deviation, and a 0.2Sv tidal modulation. The mean transport is about twice as large as that obtained by Tessler et al. (2010) from mooring data at the sill. This discrepancy is within our uncertainties. An explanation for it is that our time-averaged velocity section (Fig. 6c) reveals an intensified current to the western side of the Sill. This agrees with a southward density-driven flow along the Mindoro-Panay Strait system and momentum advection in approximate balance with the Coriolis force and bottom stress, with the former deflecting the flow to the right. This finding of western-side intensified flow agrees with hydrographic data (Tessler et al., 2010), but could indicate that the transports at the sill underestimate total transport. On the other hand, if we were to restrict our bottom transport to salinities within 34.43 to 34.46, we would divide our estimates by more than two. In the Sibutu Strait, we find a deep flow (Fig. 6d) with strong tidal velocities, but a small net time-averaged inflow of 0.032 Sv into the Sulu Sea during Feb-Mar 2009. Also visible are periods of intense instantaneous deep inflow from the Sulawesi, modulated by spring and neap tides, at around twice a month to a month frequency. This is confirmed by the salinity at the strait section (Fig. 6a) spatially-averaged within 20m of the bottom (Fig. 6e); the deep mean salinity at Sibutu is indeed driven by such slower frequencies, increasing to 34.59 in periods of inflow from the Sulawesi.

To confirm that these two straits are the two main sources for the deep salty Sulu water, we examine the overflows from deep depths. Fig. 7a shows the salinity integrated vertically (200-1000m), but only if the salinity is 34.45 to 34.55, and averaged over Feb. 4-11, 2009. The corresponding integrated and averaged horizontal velocity is shown on Fig. 7b. Clearly visible are the Mindanao current advecting higher salinities from the sub-surface Pacific waters to the Sulawesi, which can ultimately reach the Sibutu. Also shown are the smaller but still sufficient salinities of the South China Sea, which flow in the Mindoro-Panay Strait system. The Panay Sill provides averaged salinities around 34.47 to 34.52 while the Sibutu provides averaged salinities around 34.5 to 34.55, with mixing occurring with each strait. Also shown are upwelling along the steep shelfbreaks in the region. The tidally active Balabac Strait (sill depth around 100m) could at times be a source, but our present simulations did not show significant inflow events. Visible in the Sulu Sea just north of Sibutu and the Sulu Archipelago (Fig. 7a) are strong internal tides/waves signals suggesting a mechanism for deep mixing. This is required since the highest mean salinities in the Sulu Sea are below 1000m.

In Fig. 7c,d, we illustrate the mixing and upwelling/downwelling patterns occurring at Sibutu. Within the 100 to 200m layer, two water masses collide and can be tidally mixed at the sills of Sibutu: the sub-

surface modified salty Pacific waters advected in from the Sulawesi and the sub-surface waters of the Sulu Sea (less salty at those depths in part due to inflow of more-modified Pacific waters from the South China Sea). We show in Fig. 7c,d that deep waters below 700m can upwell to 200m, mix within the complex Sibutu Strait sills and sub-basins, and finally flow into the Sulu Sea. These waters can either downwell, further mixing along the steep Sulu bathymetry, or advect on the narrow shelves of the Sulu Archipelago. The vertical velocity patterns shown (Fig. 7d) oscillate with tides (of different phases on each side of the strait) and are not permanent. However, the neap and spring cycles lead to periods favorable to mean upwelling from the deep Sulawesi (see Fig. 6e). We find that mixing occurs at the entrance of Sibitu and at the exit of Sibutu within internal waves, but we also discover stronger internal waves all along the steep shelfbreak on the northern side of the Sulu Archipelago (Fig. 7e,f). Several of these waves would develop into deep solitons in the real ocean. We note that the northern Sibutu and Sulu Archipelago shelfbreak waves are not in phase, but that stronger tidal events occur every 14 days or so at both locations. These events lead to vigorous mixing of the high salinity waters (not shown). To illustrate the circulation and mixing in the Sulu Sea, we show the depth of the surfaces of constant potential density anomaly $\sigma_\theta=26.15$ and $\sigma_\theta=26.50$ (Fig. 7g,i), and the salinity fields on the two surfaces (Fig. 7h,j), all estimated on Feb. 20 at 1930Z. The inflow from the Mindoro-Panay Strait system is clearly visible (Fig. 7h). At Sibutu, but even more so along the Sulu Archipelago, several trains of internal waves have developed (compare with the first week of Feb. on Fig. 7a). As the saltier waters are mixed down at depth, they form a tongue of higher salinity on which other deeper internal waves can ride, further increasing the mixing. Note that these deeper internal waves travel at an angle from the Sulu Archipelago (e.g. Fig. 7h). The salinity tongue also creates horizontal density gradients which displace the overall cyclonic circulation further offshore, ultimately creating anticyclones on both sides of the tongue. The depth of $\sigma_\theta=26.50$ (Fig. 7i) reveals a main driver for this tendency towards cyclonic circulation in the Sulu Sea, the sinking, mixing and advection of heavier salty waters along all of its slopes. The highest salinities on $\sigma_\theta=26.50$ (Fig. 7j) confirm the advection form Sibutu. The strongest mixing and sinking occurs at the steep shelfbreak in the middle of the Sulu Archipelago: salinity on $\sigma_\theta=26.55$ indicates that it is the fastest there, reaching a depth of 1800m in 3 weeks.

Statistical Field Estimation for Complex Coastal Regions and Archipelagos: A manuscript on our new OA schemes based on estimating the length of shortest sea paths using LSM and FMM is ready to be submitted (Agarwal and Lermusiaux, 2010). These schemes could improve widely-used gridded databases such as the climatological gridded fields of the World Ocean Atlas since these oceanic maps were computed without accounting for coastline constraints. We showed the need of using our new schemes in complex regions, where climatologies provide unrealistic estimates of water column characteristics by mixing historical data from geographically and temporally disparate sources.

Idealized Simulations and Dynamics with Finite Element Methods

We found (Ueckermann et al., 2010) that both quadrature-based and quadrature-free discretizations give accurate, convergent results in areas where the field is well-resolved. We also found that a curved boundary mesh is necessary for accurate advection over topography using high-order schemes. We found that numerical oscillations due to discontinuities in tracer concentrations can be significant for both low and high order schemes. Our results showed that low-order temporal discretizations allowed rapidly growing numerical errors, unsatisfactory for certain biological applications. Finally, by quantitatively evaluating the truncation error and smoothness of solution fields, we found that higher-order spatial discretizations are more accurate in regions where the solution is smooth.

IMPACT/APPLICATIONS

This research will contribute to coastal physical and biogeochemical oceanography in general and dynamics of Straits in particular. This will increase capabilities of navy operations in these regions, especially the surveillance of transit routes, safety of man-based activities, management of autonomous vehicles, and overall tactical and strategic decision making under uncertainties in sensitive areas.

TRANSITIONS

Interactions and coordination are ongoing with several investigators and teams involved with this DRI, specifically with observational efforts, and numerical and theoretical modeling investigations. Our model forecasts and re-analyses NetCDF files have been made available to the whole team. Simulations results, topography field estimates and transport estimates have been shared with A. Gordon and Z. Tessler from the Lamont Doherty Earth Observatory. In additions, simulation results have been shared with K. Mohseni and D. Lipinski from the University of Colorado.

RELATED PROJECTS

Collaborations occur under the ONR grant "Physical and Interdisciplinary Regional Ocean Dynamics and Modeling Systems" (N00014-08-1-1097).

REFERENCES

Cockburn, B., Gopalakrishnan, J., and Lazarov, R., 2009. Unified hybridization of discontinuous galerkin, mixed, and continuous galerkin methods for second order elliptic problems. Siam Journal on Numerical Analysis, 47(2):1319-1365.

Guermond, J.L., Minev, P., and Shen, Jie, 2006. An overview of projection methods for incompressible flows. Comput. Methods Appl. Mech. Engrg, 195:6011-6045

Hesthaven, J.S., and Kirby, R.M., 2008. Filtering in legendre spectral methods. Mathematics of Computation, 77(263):1425-1452.

Hoteit, H., Ackerer, Ph., Mosé, R., Erhel, J., and Philippe, B., 2004. New two-dimensional slope limiters for discontinuous Galerkin methods on arbitrary meshes. Int. J. Numer. Meth. Engng, 61:2566-2593.

Mavriplis, C.A., 1989. Nonconforming Discretization and a Posteriori Error Estimators for Adaptive Spectral Element Techniques. PhD thesis, MIT.

Nguyen, N. C., Peraire, J., and Cockburn, B., 2009. An implicit high-order hybridizable discontinuous galerkin method for linear convection-diffusion equations. J. Comp. Physics, 228(9):3232-3254.

Reed, W. H. and Hill, T. R., 1973. Triangular mesh methods for the neutron transport equations. Los Alamos Scientific Laboratory Report LA-UR-73-479.

Tessler, Z., A.L. Gordon, L.J. Pratt, J. Sprintall, 2010. Transport and Dynamics of Panay Sill Overflow in the Philippine Seas, J. Phys. Oceanog., in press.

PUBLICATIONS

Haley, P.J., Jr. and P.F.J. Lermusiaux, 2010. Multiscale two-way embedding schemes for free-surface primitive-equations in the Multidisciplinary Simulation, Estimation and Assimilation System. Ocean Dynamics. doi:10.1007/s10236-010-0349-4, In press.

Lermusiaux, P.F.J. P.J. Haley, Jr., W.G. Leslie, A. Agarwal, O. Logutov and L.J. Burton, 2011. Multiscale Physical and Biological Dynamics in the Philippines Archipelago: Predictions and Processes. Oceanography, Special PhilEx Issue, Submitted.

Ueckermann, M.P. and P.F.J. Lermusiaux, 2010. High Order Schemes for 2D Unsteady Biogeochemical Ocean Models. Ocean Dynamics. In press, doi:10.1007/s10236-010-0351-x.

Ueckermann, M.P., Lermusiaux, P.F.J., and Haley, P.J., Jr., 2010. High Order Discontinuous Galerkin Schemes for Coupled Physical-Biogeochemical Ocean Modeling. 9th International workshop on Multiscale numerical Modeling for coastal, shelf, and global ocean dynamics. Cambridge, Ma.

Presentations and publications are available from the MSEAS web-site. Specific figures are available upon request.

FIGURES
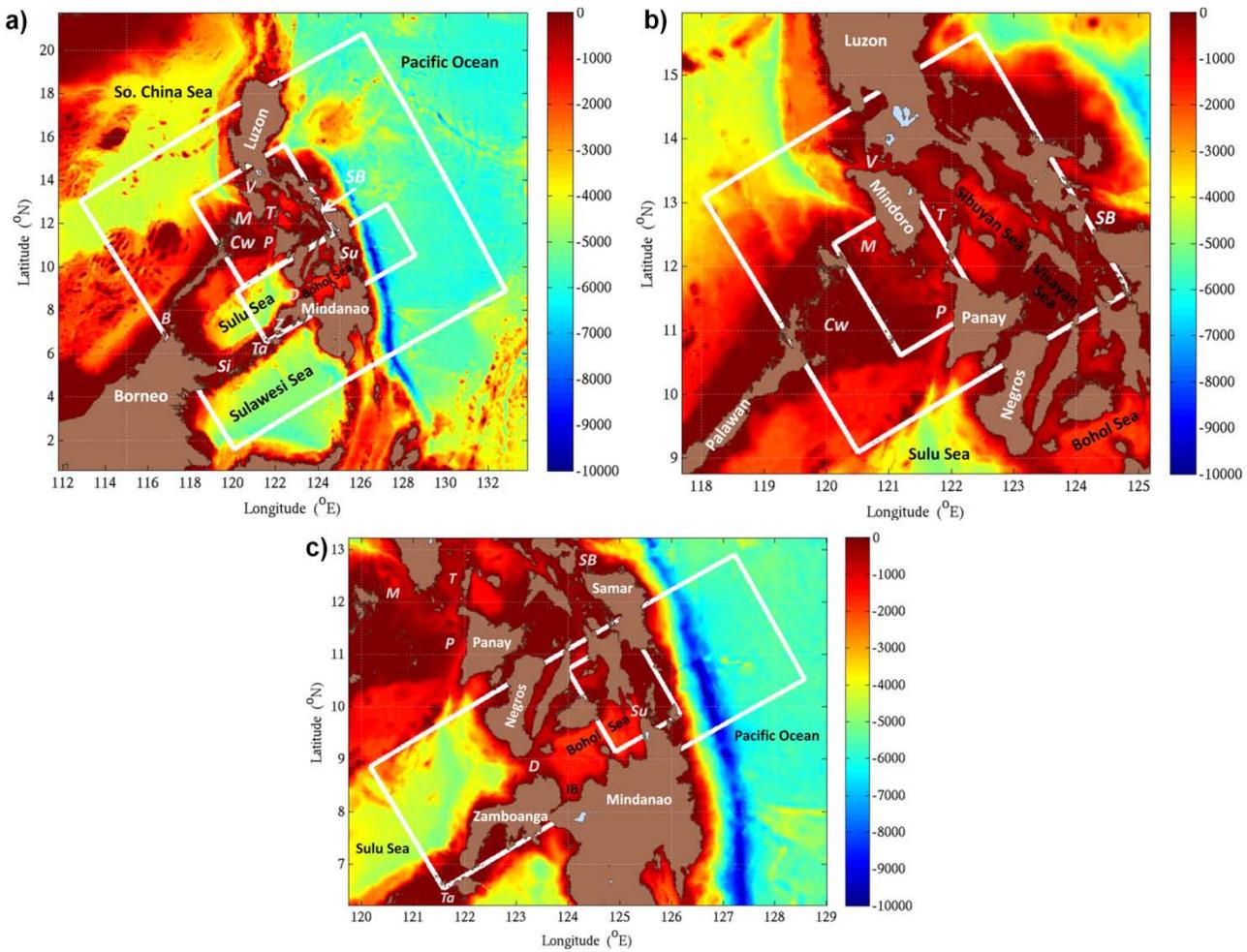
Figure 1 – Spherical-grid domains in a telescoping zoom configuration for our multiscale simulations in the Philippine Archipelago overlaid on our estimate of bathymetry (combining V12.1 of the Smith and Sandwell topography with hydrographic and bathymetric ship data). a) Archipelago 9km resolution domain with nested Mindoro (3km) and Mindanao (3km) domains. b) Mindoro Strait 3km and 1km domains. c) Mindanao/Surigao Strait 3km and 1km domains. Straits and local features are identified by one or two-letter abbreviations. Alphabetically these are: B – Balabac Strait, Cw – Cuyo West Passage, D – Dipolog (Mindanao) Strait, IB – Illigan Bay, M – Mindoro Strait, P – Panay Sill, SB – San Bernardino Strait, Si – Sibutu Strait, Su – Surigao Strait, T – Tablas Strait, V – Verde Island Passage, Ta – Tapiantana Strait, Z – Zamboanga Strait
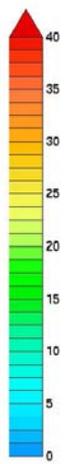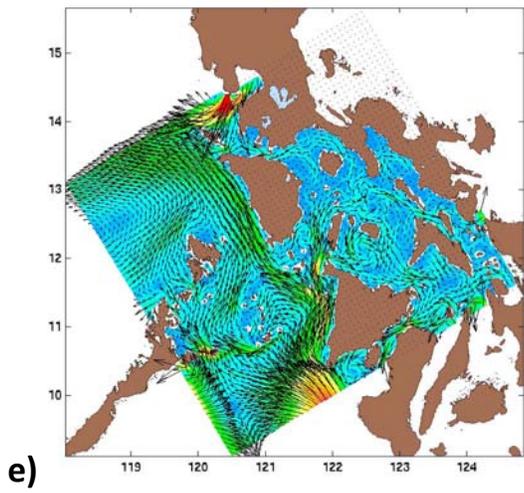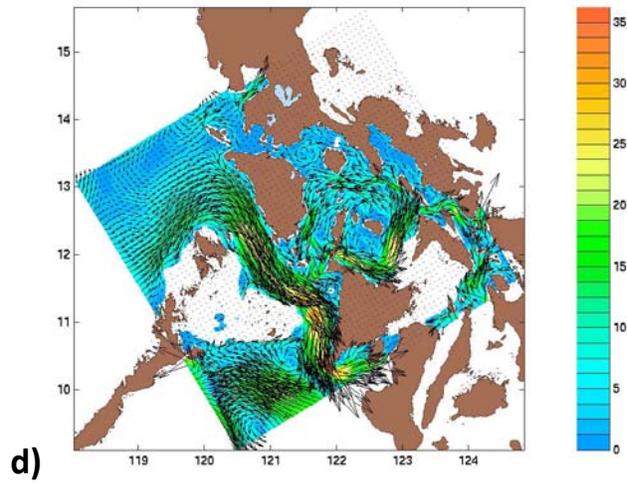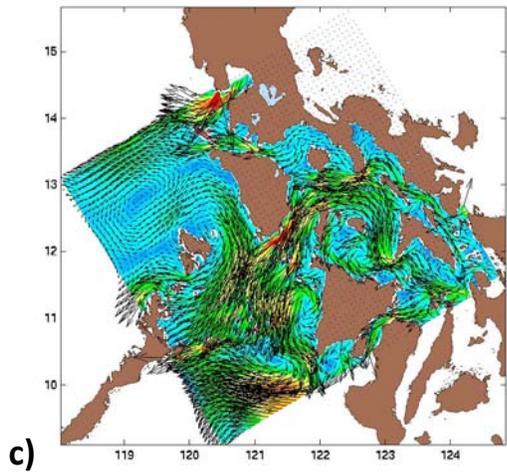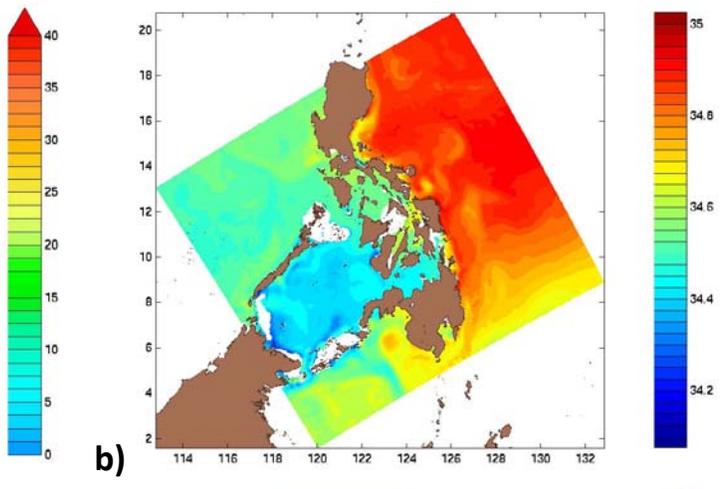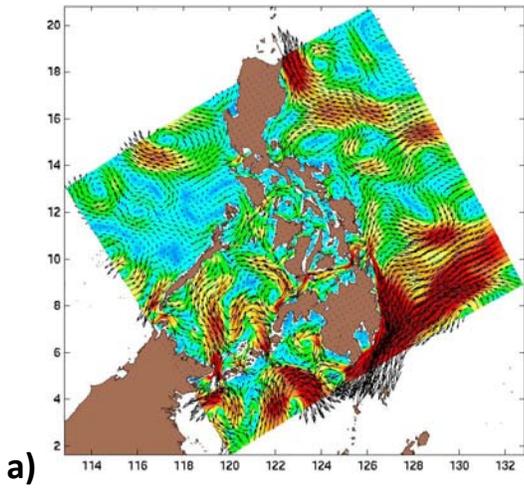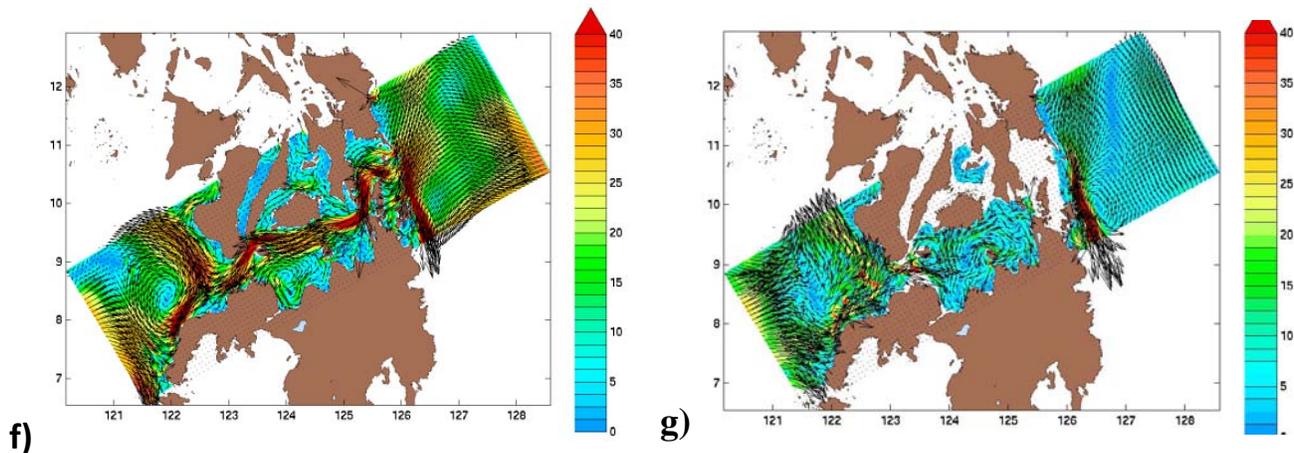
Figure 2 - Time and depth averaged model re-analysis estimates displaying canonical flow features for PhilEx-09. (a) Velocity averaged between 0-100m during 18-25 Feb; (b) Salinity averaged between 100-200m during 18-25 Feb; (c) Velocity in Mindoro domain averaged between 0-50m during 18-25 Feb; (d) Velocity in Mindoro domain averaged between 100-200m during 18-25 Feb; (e) Velocity in Mindoro domain averaged between 0-50 m during 18-25 Mar; (f) Velocity in Mindanao domain averaged between 0-100m during 18-25 Feb; (g) Velocity in Mindanao domain averaged between 400-500m during 18-25 Feb.
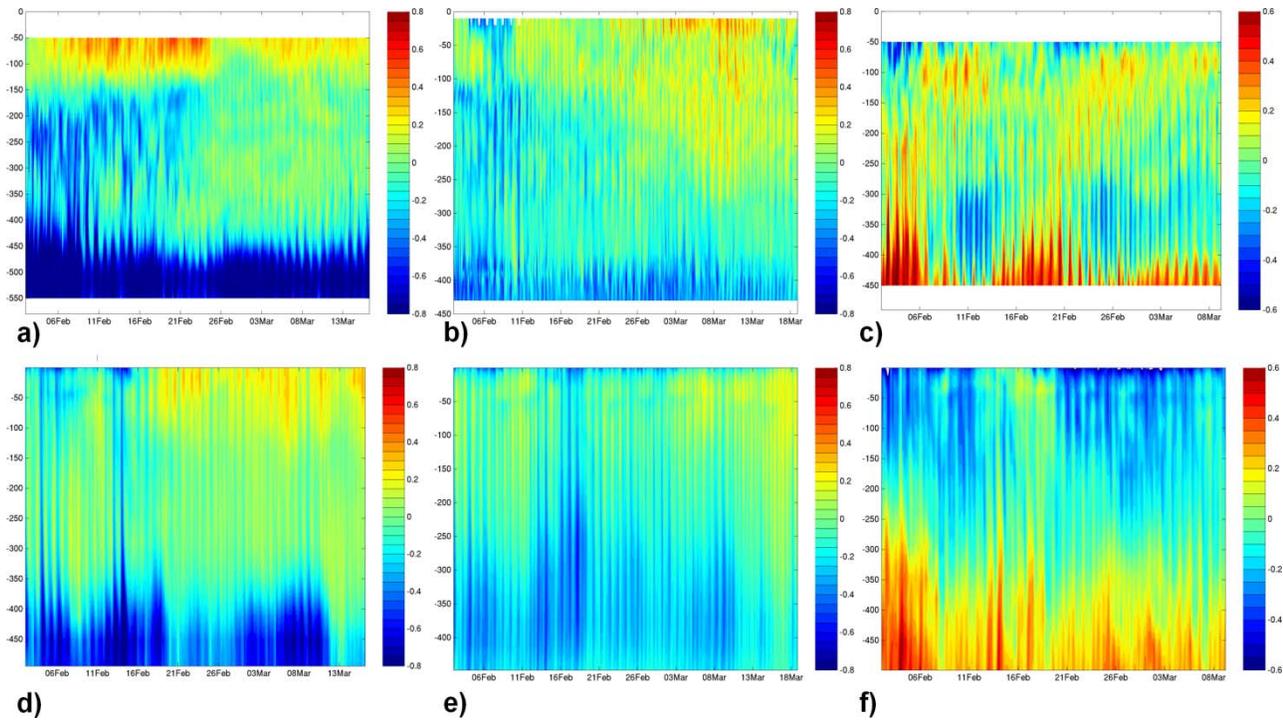
Figure 3 – Comparison of observed and modeled along-strait velocity over the period 2 Feb. 2009 until the recovery of each individual mooring. The top row is observations at moorings – a) Panay, b) Mindoro, c) Dipolog. The bottom row is model re-analysis estimates – d) Panay, e) Mindoro, f) Dipolog. The model estimates are in generally good agreement with the features of the observed flows, e.g. the bottom intensified flows especially at Panay and Dipolog, that even though no synoptic in situ data is utilized in the re-analysis.
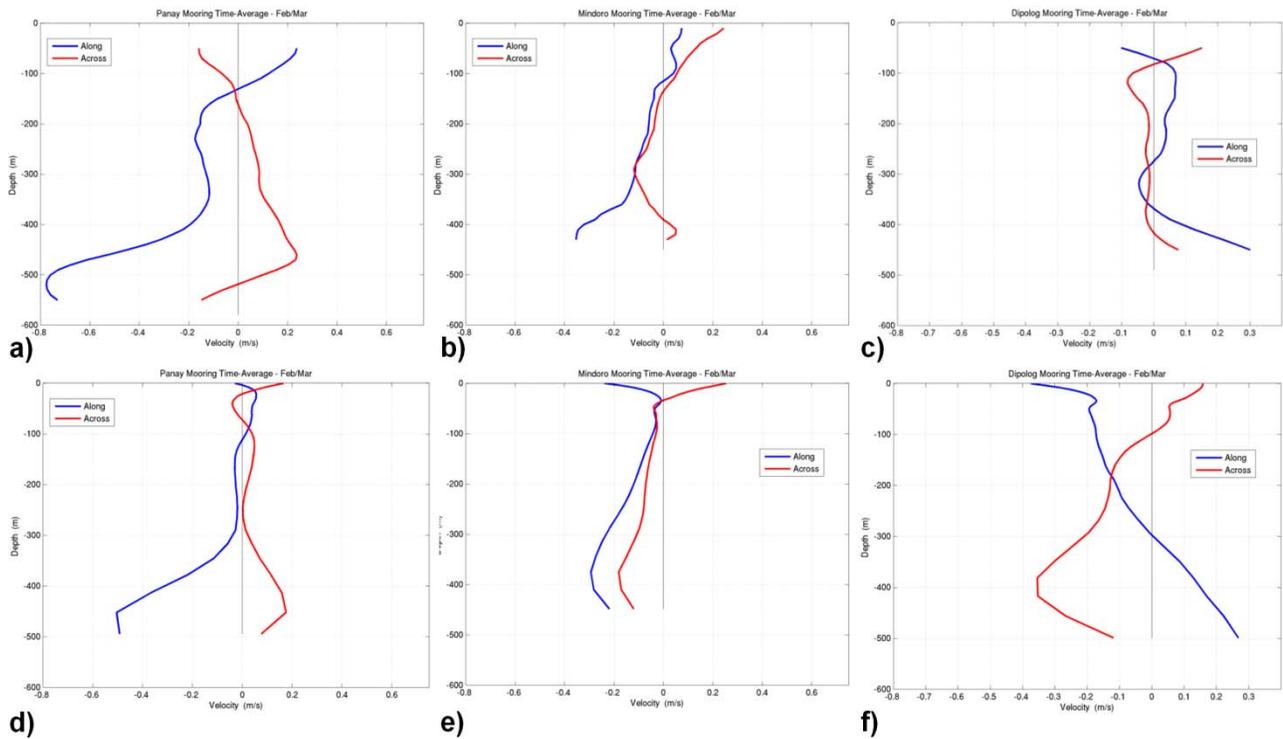
Figure 4 – Comparison of time-averaged along-strait (blue) and across-strait (red) velocities over the period 2 Feb. 2009 until the recovery of each individual mooring. The top row is observations at moorings – a) Panay, b) Mindoro, c) Dipolog. The bottom row is model re-analysis estimates – d) Panay, e) Mindoro, f) Dipolog. Even though no in situ data is assimilated, the structures of the simulated mean profiles overall agree with that of the observed means.
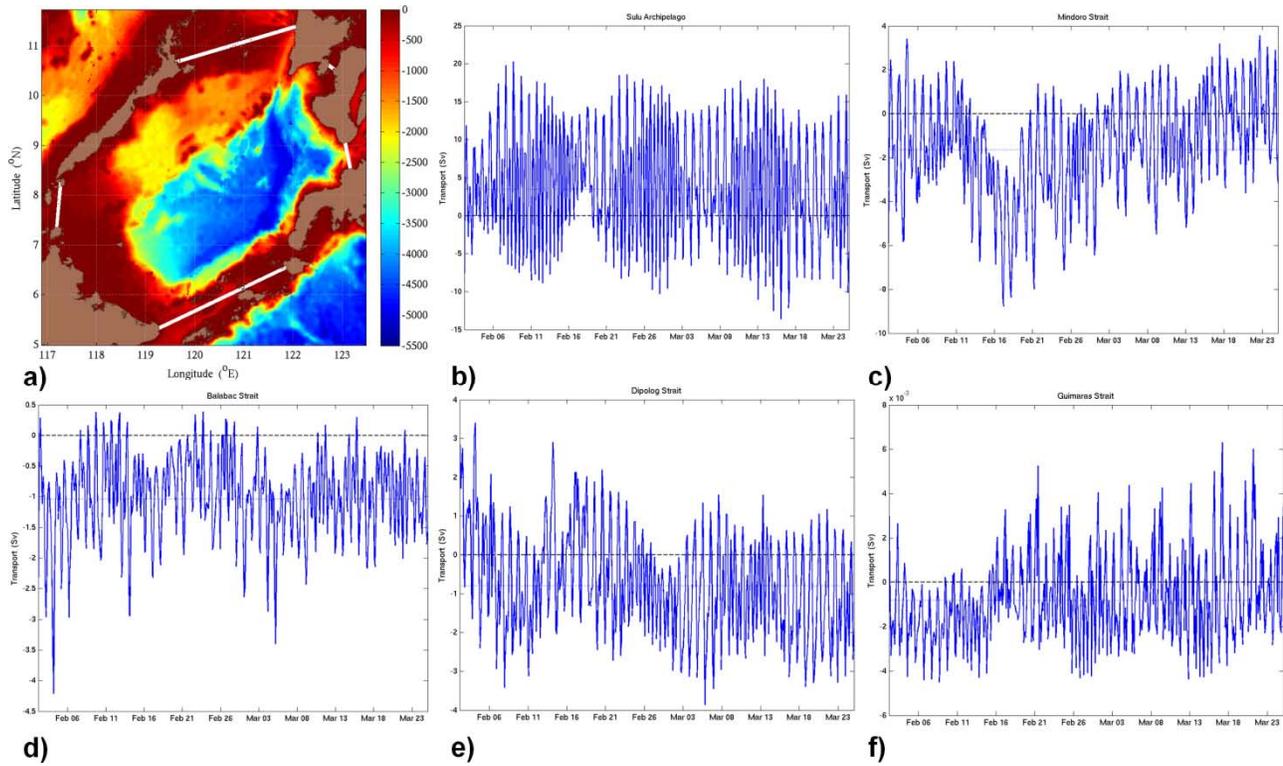
Figure 5 – Transports into and out of the Sulu sea (positive transports are out of the Sulu sea, for an outward normal) during Feb.-Mar. 2009. (a) Locations of the sections through which transports are evaluated, then transports as a function of time through the: (b) Sulu archipelago (+3.47 Sv time-average); (c) Mindoro strait (-1.65 Sv time-average); (d) Balabac strait (-1.04 Sv time-average); (e) Dipolog strait (-0.79 Sv time-average); and (f) Guimaras Strait(-8×10^{-4} Sv time-average).
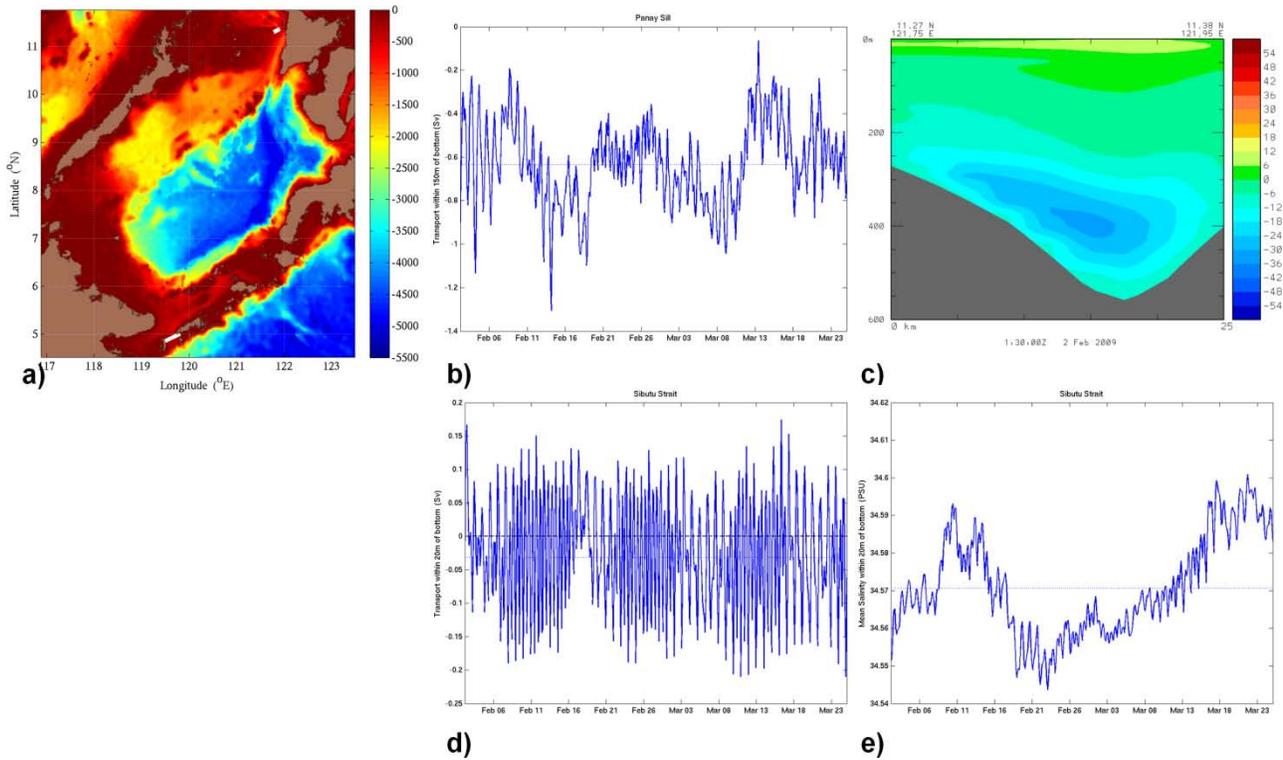
Figure 6 – Bottom water transports (Sv) over the Panay Sill and through the Sibutu Strait during Feb.-Mar. 2009. Positive transports are out of the Sulu Sea (outward normal). (a) Locations of sections for the Panay Sill proper and Sibutu Strait; (b) Transport versus time, over the Panay Sill within 150m of the bottom, providing a net time-average inflow of 0.645 Sv into the Sulu, with a 50% uncertainty standard deviation; (c) Velocity (cm/s, positive into the page), averaged over time during February-March 2009, over the Panay Sill, showing the westward deflection of the southern density-driven flow by the Coriolis force; (d) Transport versus time in the Sibutu Strait within 20m of the bottom, showing a small net time-average inflow of 0.032 Sv into the Sulu Sea; and (e) Mean salinity versus time in the Sibutu Strait within 20m of the bottom.
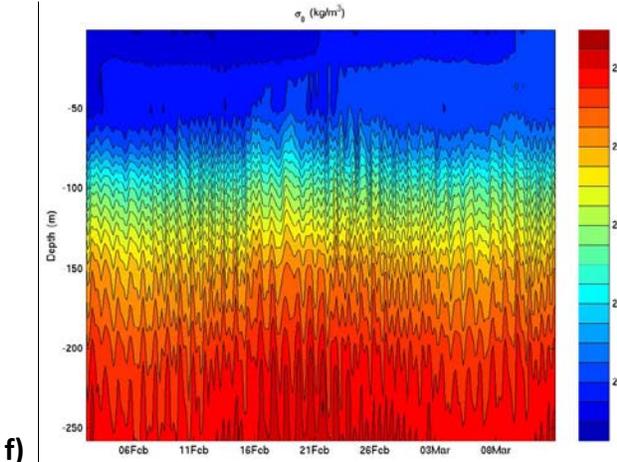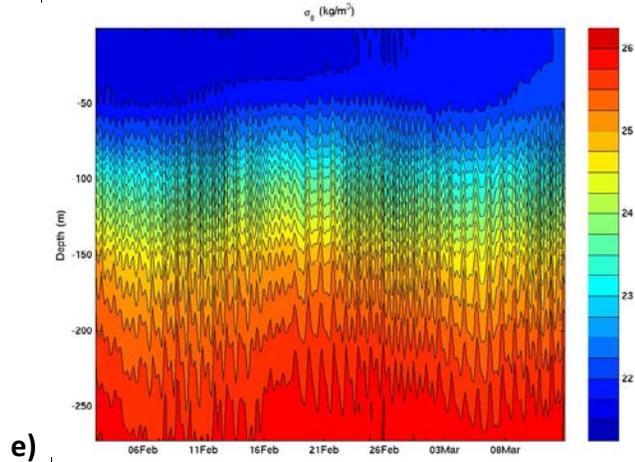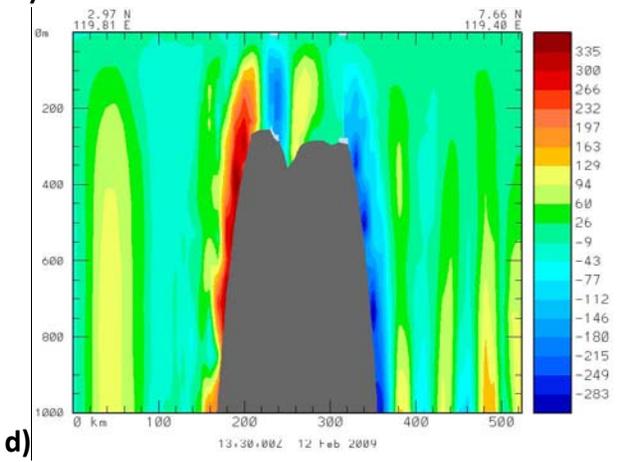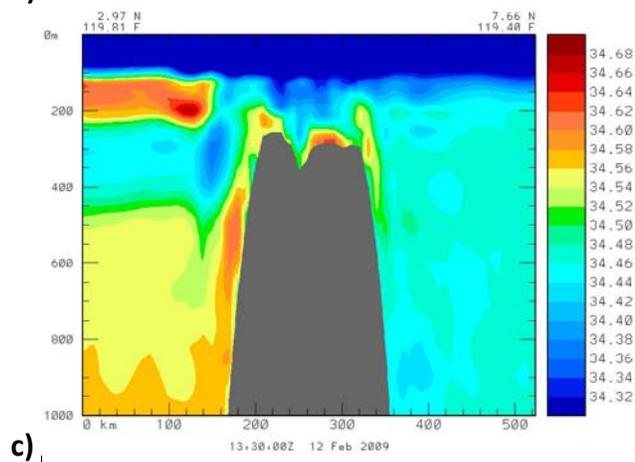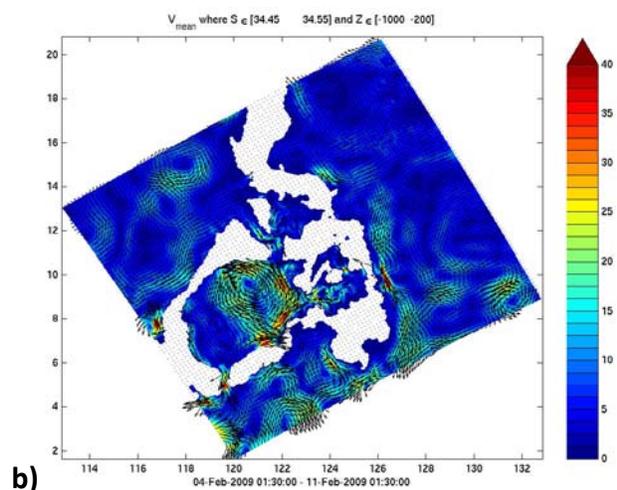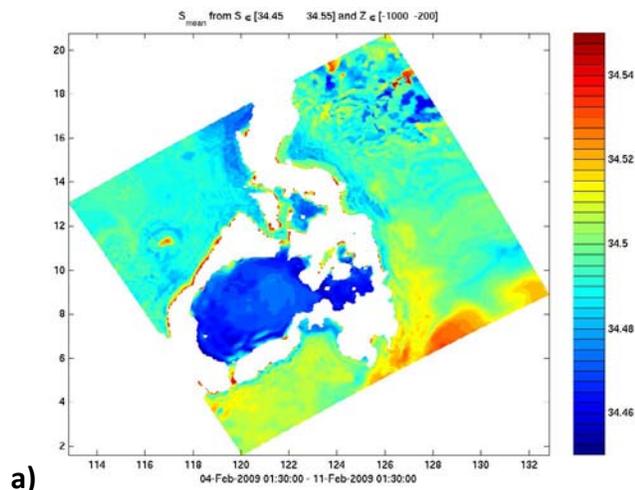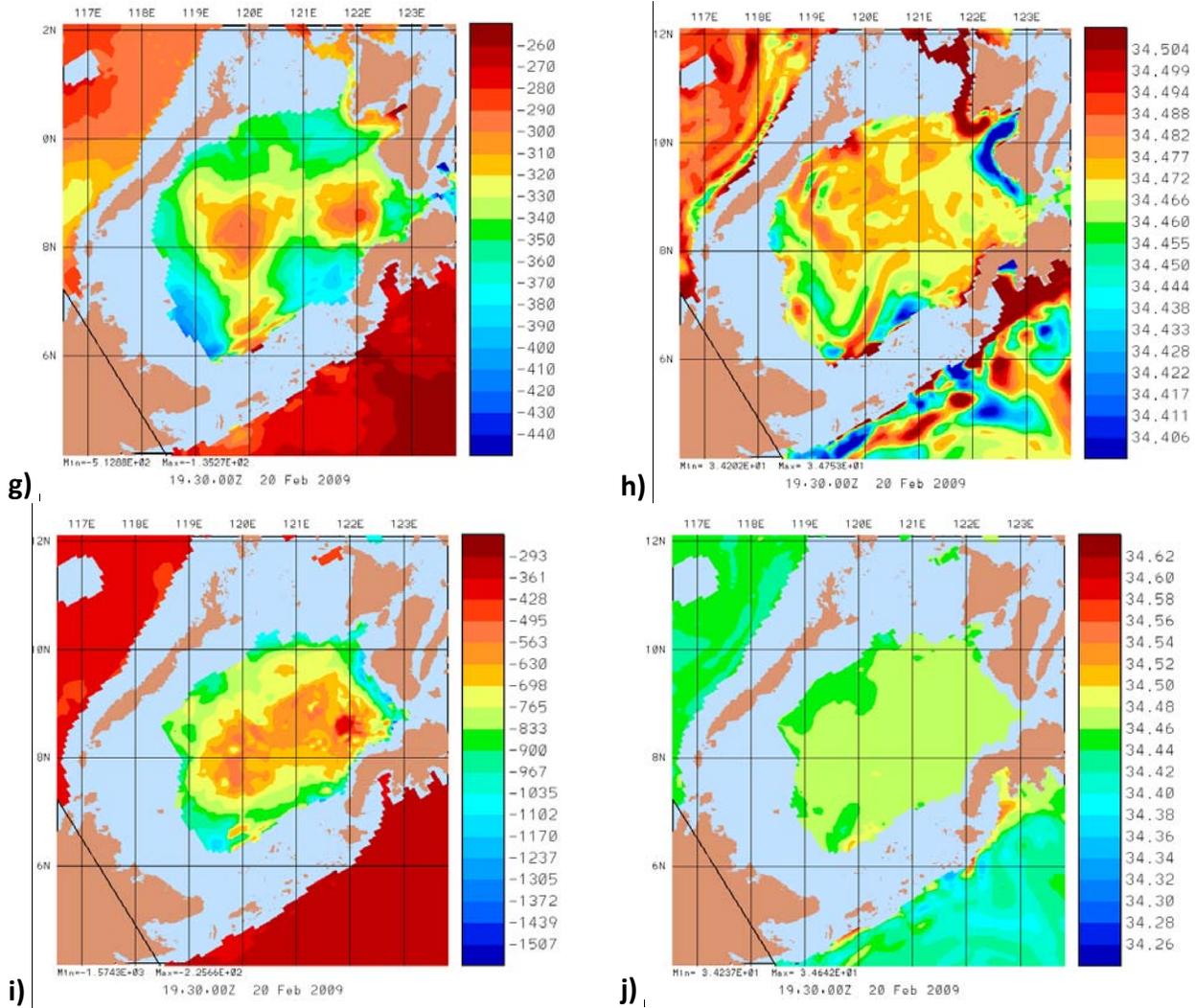
Figure 7. (a): Simulated salinity vertically-averaged from 200m to 1000m depths, but only if the salinity is within 34.45 to 34.55 (salinities outside that range are not considered), and temporally averaged over Feb. 4 to 11, 2009. (b): Corresponding vertically-integrated and temporally averaged horizontal velocity (cm/s). (c) and (d): Salinity and vertical velocity (m/day) snapshots, in a section along the Sibutu Strait from the Sulawesi to the Sulu, as estimated on 13:30Z, Feb. 12, 2009. (e) and (f): Potential density anomalies σ_θ as a function of time during Feb. 2 to Mar. 13, 2009, at the northern edge of Sibutu (5.8^oN, 119.5^oE) and at the steep northern shelfbreak of the Sulu Archipelago (6.2^oN, 120.3^oE), respectively. (g) and (h): Depth of the surface of constant potential density anomaly $\sigma_\theta=26.15$ and the salinity on this surface, respectively, both estimated for 19:30Z on Feb 20, 2009. (i) and (j): as (g) and (h), but for the density anomaly $\sigma_\theta=26.50$.

17